DESIGN CONSIDERATIONS FOR ULTRA-PRECISION MAGNETIC BEARING SUPPORTED SLIDES[1]

Alexander H. Slocum
Massachusetts Institute of Technology
Cambridge Massachusetts

David B. Eisenhaure
SatCon Technology Corporation
Cambridge Massachusetts

SUMMARY

This paper describes development plans for a prototype servo-controlled machine with 1 Ångstrom resolution of linear motion and 50 mm range of travel. Two such devices could then be combined to produce a two dimensional machine for probing large planar objects with atomic resolution, the Ångstrom Resolution Measuring Machine (ÅRMM).

INTRODUCTION

Several Ångstrom resolution devices currently exist. Scanning electron microscopes (STMs) are flexural linkage structures with Ångstrom resolution and range of motion only on the order of one micron [1]. Because of its small range of motion, an STM can be made small enough to make it virtually immune to thermal and vibration problems that would plague a machine with centimeter range of motion. Researchers at the National Physical Laboratories (NPL) in England have built a linear stage with 1 Å smoothness of motion over a range of centimeters. The stage uses Rulon™ pads as bearings that are arranged kinematically on a Vee way [2]. However, questions regarding long term stability of the plastic bearings and controllability in the presence of sliding friction remain unanswered. Current designs of other precision machines such as wafer steppers and diamond turning machines [3] are principally performance limited by mechanical contact between moving parts, misalignment between actuators and bearings, bearing stability, and attainable temperature control [4,5,6]. To help overcome these problems, coarse-fine positioning system have evolved as shown in Figure 1. Although they can

[1] This work was supported by the Center for Manufacturing Engineering of the National Bureau of Standards.

be effective, they are mechanically cumbersome and are intrinsically difficult to control. The design envisioned for the ÅRMM would address these issues by way of its kinematic magnetic bearing design.

The design of the ÅRMM evolved into the crossed axis design shown in Figures 2-4. A two axis version only requires fabrication and installation of a "mirror image" of the first axis. The resultant two axis machine would have a spherical or cubic shape to maximize structural efficiency with respect to stiffness and thermal stability. The axis' moving structural members would be mirror finished and be used as reflectors for the laser interferometers that provide position feedback signals to magnetic bearings[2]. The magnetic bearing actuators would be configured kinematically: Five magnetic bearing actuators positioned to control five degrees-of-freedom.

TEMPERATURE CONTROL

Controlling system temperature without introducing large gradients could be achieved by using constant or low power devices[3], operating the system at a steady thermal state, and configuring the system as a sphere hanging inside another temperature controlled evacuated sphere. The two spheres would be radiantly coupled with the outer sphere cooled by a high velocity coolant source[4].

Temperature control by radiant coupling can be effective and is not as prone to the formation of gradients as convective cooling is. Consider the heat transferred between two bodies by radiation:

$$Q_{net} = F_{1\text{-}2}\,\sigma A_1(T_1^4 - T_2^4) \qquad (1)$$

If 10 watts of waste heat are to be removed from 1.0 or 0.5m diameter spheres, and temperature is to be maintained at 20°C (293 °K), then Equation 1 can be used to determine that corresponding outer spheres must be kept at 19.440407°C and 17.742068°C respectively.

Assuming steady state conditions, small deviations δT (less than 0.1°C) in the temperature of the outer sphere will affect the amount of power retained by the inner spheres by:

$$\Delta Q_{watts\ @\ 0.25m,\ 17.742068\ C} = 4.378 * \delta T \qquad (2)$$

$$\Delta Q_{watts\ @\ 0.5m,\ 19.440407\ C} = 17.820 * \delta T \qquad (3)$$

---

2 The axis would be designed so servo forces from the bearings and the weight of the part caused less than 0.1 Å deformation.

3 For example, magnetic bearings with heaters, piezoelectric actuators, and laser interferometers.

4 The inner sphere cannot be cooled directly because the high velocities needed to eliminate gradients also generate turbulence and vibration.

If deviations in the outer sphere temperature occur with a time constant much faster than that of the inner sphere, then the thermal mass of the inner sphere will prevent it from being affected by these variations.

In order to make a first order evaluation of various materials for the ÅRMM structure, consider the time it takes the inner sphere (δT_i) to reach a new equilibrium temperature given a step change in the outer sphere temperature. Assume that the new equilibrium temperature is $T_{inominal} + \delta T_i$, where δT_i is the change in temperature that causes 0.1Å thermal growth in a 0.25m segment of the structure. Given a change in the outer sphere temperature of δT_o, then to the first order the time it takes the inner sphere to change its temperature by δT_i via radiant coupling is

$$t = \frac{R_1 C_p \delta T_i}{3F_{1-2}\sigma[T_{inom}^4 - T_{onom}^4 - (T_{inom}+\delta T_i)^4 + (T_{onom}+\delta T_o)^4]} \quad (4)$$

Table 1 illustrates this change for various candidate materials. Based on the time evaluation, Zerodur or Invar should be used. If the thermal diffusivity is considered, a material such as copper should be used in order to minimize gradients[5].

By tuning power dissipation and the equivalent black body view factor with the size of the sphere, it may be possible to utilize an inexpensive accurate temperature control process (i.e. a phase change process) for controlling the inner sphere's temperature. For example, assume the outer sphere is contained in an ice water bath and the temperature of the outer sphere is fine tuned with an electric heater. If the inner sphere still needs to dissipate 10 Watts of power, the diameter of the inner sphere should be about 0.1758 m if the spheres still behave like black bodies.

This preliminary analysis gives a good indication of where to start the design process, although it does not include transient affects nor does it model hot spots within the sphere. Hot spots can be prevented if the structure is suitably instrumented and zone temperature control is used.

BEARING DESIGN

The properties desirable in a bearing for the ÅRMM include: 1) repeatability, 2) low friction, and 3) high stiffness. Only magnetic bearings have the potential to meet these requirements, *and allow for easy adjustment of performance after fabrication.*

---

5 Zerodur, Invar, Copper, Aluminum, Beryllium and Cast Iron are all known to have very stable forms [7].

A simple magnetic bearing control system is shown in Figure 5 and is characterized by the gain (stiffness) which relates errors in position to applied magnetic force and the bandwidth which indicates the frequency range over which the magnetic force may be applied to reject disturbance forces. The magnets have negative spring constants which lead to a minimum required system bandwidth for stability of about 10 Hz for many suspensions. Maximum achievable bandwidths range from 100 Hz for a simple attractive-type system to 40 KHz or higher for systems implemented with ferrite or voice coil actuators.

At low frequencies, performance is determined almost completely by the ability of the controller to cancel disturbances. The primary control system parameter affecting disturbance cancellation is the controller gain which determines suspension stiffness. The higher the suspension stiffness, the greater the ability to reject force disturbances. Depending on the nature of the source, at high frequencies, the disturbance forces are generally absorbed by the platten's inertia and internal damping characteristics.

Figures 6 and 7 show the achievable resolution at various disturbance force levels as a function of suspension stiffness and bandwidth, respectively. The disturbance force represented is modeled as a broad band disturbance over the entire frequency range of interest. For the simple control system considered, the bandwidth is equal to the natural frequency of the system.

The principal disturbance forces acting on the slide in a laboratory environment are caused by air currents, acoustic disturbances, ground plane motion, and linear actuator error motions. Figures 8 and 9 show the disturbance forces for impinging air flow and acoustic disturbances respectively. Figure 10 shows the disturbance forces as a function of base motion for various suspension gaps. A comparison of Figures 8 through 10 shows that base motion is the largest single contributor to slide disturbance force[6]. If necessary, the sensitivity to base motion could be reduced by one order of magnitude by incorporating magnetic flux feedback in the control loop and by two orders of magnitude by employing voice coil-type actuators. Even without these changes, the total disturbance force level should be kept below about 0.01 N (0.005 lb).

Capacitance probes or laser interferometers can be used to make ultra precision measurements of the magnetic bearing gap. Regardless of

6 The current state of the art of vibration control centers on active (servo) control of vibrations [8,9,10,11], and commercially available servo-controlled systems capable of keeping table motion amplitudes below 100Å @ 10 Hz have recently become available from Barry Control and Newport Corp.

the system used, however, *a through the bearing measurement method* must be used. This maintains accuracy of the kinematic model and provides for checking measurement closure should direct measurement of the position and orientation of a region of the slide also be made.

If a laser interferometer system is used as a position feedback sensor, as shown in Figure 11, then the platten must be polished to optical quality. The cost of a laser interferometric measurement system is on the order of $10,000 per measurement axis. It is envisioned that in the near future the resolution of differential plane mirror interferometers will approach the one Ångstrom level[7]. Hence a single magnetic bearing supported slide would require $50,000 worth of laser interferometers.

For substantially less cost, on the order of $3,000 per axis, capacitance probes, also shown in Figure 11, could be used. They have the advantage of not requiring the surface of the slide to be optically polished. The finite area of their measuring tips creates an averaging effect which reduces the effect of surface finish errors on the gap measurement. However, on the Ångstrom level, long term drift problems may render the probes inadequate for continuous operation of the system over a period of days.

ACTUATORS

There are numerous actuator possibilities for the ÅRMM, especially if one considers combinations of macro and micro motion systems. However, because of the complexity of a coarse-fine actuator system, only linear electric motors, and piezoelectric inchworm translators are considered here.

Linear electric motors have had a practical resolution limit on the order of 10 microinches, based on the fact that mechanical coupling and thermal errors in existing systems begin to dominate at this resolution. If a kinematic transmission system could filter out thermal and mechanical errors from a linear motor, then advanced measurement and control techniques may increase their applicability to ultra precision machines. Typically, linear motors are controlled by current feedback from the motor and position feedback of the slide. However, current feedback can only provide clean motor force resolution on the order of 1/4,096 - 1/65,536. Also for current feedback to be useful, the motor needs to be rigidly coupled to the slide, but this permits mechanical and thermal errors to be transmitted to the slide. Instead of current feedback from the motor, the position of both ends of the transmission system should be measured with a laser interferometer.

[7] Discussions with Carl Zanoni, VP. Eng., Zygo Corp., Middlefield, Connecticut.

Piezoelectric inchworm devices are high resolution actuators with large ranges of motion. Their resolution is a function of the increment of each step, which can be on the order of 10^{-11} meters, and how the device clamps between steps; a jerky clamping action will induce errors. Currently available piezoelectric inchworm actuators typically have a thick force transmission bar which a circumferential piezoelectric element clamps onto. Unfortunately the bar also transmits lateral "noise" forces from the actuator to the platten, and the bar can never be aligned perfectly with the platten. Typical axial resolution is on the order of 50 Ångstroms, although lateral errors can amount to microns. Cost of this system is on the order of $1,700, excluding a precision power supply[8,9].

As shown schematically in Figure 12, the wire-piezo inchworm actuator designed for the ÅRMM can deliver 0.1 Ångstrom axial resolution with less than 0.1 Ångstrom lateral error motion. Cost to manufacture this system is on the order of $6,000, excluding a precision power supply.

Design of a control system to achieve smooth jerk-free motion from any inchworm actuator is potentially very difficult. On the other hand, the advantages offered by piezoelectric inchworm devices include essentially zero thermal energy generation and virtually infinite resolution.

KINEMATIC TRANSMISSION SYSTEMS

The purpose of a kinematic transmission system is to negate the effect of non-axial motion components on the motion of a linear slide[10] by allowing members to move (i.e. slide or deflect) in non-sensitive directions. There are two principal types of kinematic transmissions: active and passive. Active systems are those that use low or zero friction bearings to accomodate errors while maintaining high axial stiffness; however, these would be too complex for use on the ÅRMM. Passive systems, on the other hand, use flexural elements to accomodate error motions, and include beam, membrane, and wire type elements as shown in Figure 13.

A wire transmission, as shown in Figure 13, is the simplest form of a kinematic transmission system and can be accurately modeled as a simple linear spring. The axial stiffness of the wire is a function of the cross sectional area A of the wire, the length of the wire ℓ, and Young's Modulus of elasticity, E: $K_{axial} = AE/\ell$. The lateral stiffness of the wire transmission, which should be minimal, is a function of the tension in the wire, the

8 New Micropositioning Products. Burleigh Instruments, Fisher, NY.

9 Physik Instrumente: The PI System Catalog. Physik Instrumente (PI) GmbH & Co. West Germany. 8/86.

10 It should also help to reduce the amount of heat transfer from the actuator to the slide via its thin cross section.

lateral error motion ε, and the length ℓ of the wire: $K_{lateral} = 2T/\ell$. By measuring the lateral motion of the wire, the ability of the transmission system to prevent non-axial forces from acting on the slide can be determined.

Typically, the tension in the wire will be on the order of 4-5N (1.0 lb), just enough to keep it taught and prevent backlash. The error motion the wire may be required to compensate for could be as large as 25μm (0.001 in), and the length of the wire on the order of 12-13 cm (5 in). With these parameters, the lateral force transmitted to the slide is only on the order of 0.0018N (0.0004 lb). If the slide has an axial stiffness on the order of 180 x 10^6 N/m (10^6 lb/in), the resultant error motion will only be on the order of 0.1 Ångstroms. However, in order for the linearized expression for lateral stiffness to be valid, the length to diameter ratio for the wire should be on the order of 500:1. Thus the axial stiffness is limited to: $K_{axial} = \pi\ell E/2.5x10^5$. For the previous example, K_{axial} = 330KN/m (1900 lb/in). In order to increase the apparent stiffness, software based control techniques are needed.

Much work has been done on control of flexible systems in an effort to control more degrees of freedom than are directly measured. For example, controlling mode shapes of large flexible structures with application to robotic and space structures [12,13]. Subsequent work focused on controlling motions of cantilevered robotic structures with the assumption that only position feedback from the joints was available. The essence of this work consisted of using analysis of joint torques to predict and correct for deformations of the robot's structural members [14,15,16,17]. This is a similar problem to that faced by kinematic transmissions; however, these control techniques could not assume the robot had end-point feedback and thus had to rely on the use of observers. The accuracy of these techniques was only a few percent which is not acceptable for precision applications. Research has also been directed at increasing the performance of monolithic piezoelectric actuator-bearing combinations, similar to ones used on STMs, but it has not addressed the issue of using the actuators in combination with very compliant flexural couplings [18, 19].

Figure 14 shows a first-order model of a linear slide, actuator, and flexural kinematic transmission system. The actuator is modeled as a force source that acts on the damped mass of the actuator and the transmission. The transmission is the dominant spring in the system which connects the motor (mass) to the slide, which is also modeled as a mass and damper. The position of the slide cannot be controlled directly as the force output from the actuator is divided amongst accelerating the motor mass, overcoming friction, and deforming the kinematic transmission spring. The

only way to accurately determine the force in the spring (transmission) with high resolution is to measure the deflection of the spring (transmission) using a laser interferometer or a capacitance probe.

SENSOR SYSTEMS

There are four principal sensor systems that need to be designed for the ÅRMM:

1) Environmental. Temperature, pressure, and humidity all need to be monitored to enable the environment to be controlled to ensure accuracy of the machine. It is anticipated that temperature control good to 0.01-0.001°C/cm will be required for the ÅRMM. In order to achieve such high resolution and accuracy, a Mach-Zehnder interferometer will probably be used.

2) Large range of motion, high resolution. For example, the axial position of the platten has to be measured with a resolution on the order of 1.0-0.1Å over a range of motion on the order of 50 mm. Differential plane mirror interferometers will probably be used for this application. Existing technology allows for resolution to $\lambda/512$ (about 10 Ångstroms).

3) Small range of motion, ultra-high resolution. For example, the lateral position of the platten, the magnetic bearing gap, needs to be measured with a resolution of 0.1-0.01Å over a range of motion on the order of 1μm. A Fabry-Perot interferometer with the capability to resolve to $\lambda/10^6$ could even be used for this type of application where one of the reference optics is moving orthogonal to the distance being measured.

4) Measuring location of atoms. For example, scanning tunneling probes need to be adapted for use on the ÅRMM. Existing technology developed for the STM could be used; however, a single probe would take many thousands of years to map a 50 mm diameter specimen. Thus multiple probe techniques would be needed.

MOTION CONTROL SYSTEM

The resolution of the signal sent by the controller to the magnetic bearing affects the total force acting on the platten. If ηx100% of the mass M of the platten is supported against gravity by permanent magnets or a constant voltage supplied to the windings, then the downward acceleration of the platten will be $(1 - \eta)Mg$. If we assume that the magnetic bearings must be able to exert at least twice the force required to levitate the mass (sans force provided by permanent magnets), in the time t between servo update times with an N bit ADC, the platten will fall an amount δ:

$$\delta = \frac{(1 - \eta)gt^2}{2^{N-2}} \qquad (5)$$

If $\eta = 0.9$, $\delta = 0.1$Å, and $N = 14$, then the maximum servo update time is 204 microseconds; and if a 32 bit DSP is dedicated to each bearing, these times are achievable. Even with a 14 bit ADC, which generally precludes the occurrence of electrical noise problems[11], 0.1Å resolution motion control is feasible.

In order to achieve even higher resolutions, superconducting coils powered by a ultra-high-accuracy microwave-superconducting-Josephson junction power supply could be used. This type of power supply has been shown by NBS researchers to produce voltages with part-per-billion resolution. Using available superconductors that operate at liquid nitrogen temperatures would require the bearings to be wrapped in an insulating blanket, liquid nitrogen passed around the coils, and an electric heater used to balance the heatflow into the structure.

CONCLUDING REMARKS

The tools for the development of the ÅRMM currently exist, and it would take about two years to construct a single axis prototype. By careful design, resolution will be increased not by a change in the mechanical design, but by advances and changes in sensor, control system, and control algorithm designs. Perhaps with the introduction of "warm" (20-30°C) superconductor technologies, new sensors and devices will become available that will push resolution limits even further.

REFERENCES

[1] G. Binnig and H. Rohrer, "Scanning Electron Microscopy", Helvitica Physica Acta, Vol. 55 (1982) pp 726-735.

[2] Lindsey, K. and Steuart, P. "NPL Nanosurf 2: A Sub-nanometer Accuracy Stylus-based Surface Texture and Profile Measuring System with a Wide Range and Low Environmental Susceptibility," 4th Int. Precision Engr. Sem. Cransfield Inst. of Tech., U.K. 11-14 May 1987 p15.

[3] R. Donaldson, S. Patterson, "Design and Construction of a Large Vertical-Axis Diamond Turning Machine", paper presented at SPIE's 27th Annual International Technical Symposium and Instrument Display, August 21-26, 1983.

---

11 High frequency electrical noise would be damped out by the inductance of the coils and the mass of the platten. Low frequency noise would be compensated for by the closed loop position servo.

[4] W. Moore, Foundations of Mechanical Accuracy. The Moore Special Tool Company, Bridgeport, CT, 1970, (e.g. pp 24-28).
[5] J. Biesterbos et al, " A Submicron I-Line Wafer Stepper", Solid State Technology, Feb. 1987, pp 73 - 76.
[6] M. Nuhn, S. Yao, B. Avrit, "I-Line Wafer Stepper Used for Low Volume Production of 0.5 Micrometer GaAs Integrated Circuits", Solid State Technology, Feb. 1987, pp 81 - 84.
[7] J. Berthold, S. Jacobs, M. Norton, "Dimensional Stability of Fused Silica, Invar, and Several Ultra-low Thermal Expansion Materials:, Metrologia 13, pp 9-16, 1977
[8] P. R. Saulson, "Vibration Isolation for Broadband Gravitational Antennas", Rev. Sci. Instrum., Vol. 55 No. 8, August 1984, pp 1315-1320.
[9] J.C. Dankowski, "Vibration-Isolation Bench for testing in Vacuum" NASA Tech Briefs, Summer 1983, p 421.
[10] J. Sandercock et al, "A Dynamic Antivibration Support", RCA Review, Vol. 46, March 1985, pp 70 - 80.
[11] R.L. Rinker, and J.E. Faller, "'Super Spring' - A Long Period Vibration Isolator", Precis. Meas. and Fund. Const., Natl. Bur. Stds. (US) Spec. Publ. 617 (1984), pp 411 - 417.
[12] W.J. Book et al, "Feedback Control of Two-Beam Two-Joint System with Distributed Flexibility," ASME Jou. Dynamic Sys. Meas. and Con. Dec. 1975, pp 424-431.
[13] R.C. Burrows, T.P. Adams, "Control of a Flexibly Mounted Stabilized Platform," ASME Jou. Dynamic Sys. Meas. and Con. Sept. 1977, pp 174-182.
[14] R. Luh et al, "Resolved Acceleration Control of Mechanical manipulators", IEEE Tans. Auto. Cont., Vol. AC-25, 1980, pp 468-474.
[15] J. Slotine and S. Sastry, "Tracking Control of Nonlinear Systems using sliding surfaces with applications to robot manipulators", Int. Jou. Cont., Vol. 38 1983, pp 465-492.
[16] L. Sweet and M. Good, "Re-definition of the Robot Motion Control Problem: Effects of Plant Dynamics, Drive Systems Constraints, and User Requirements", Proc. 23rd IEEE Conf. Decis. and Cont., Las Vegas Nev., Dec. 1984, pp 724-731.
[17] E. Rivin, "Effective Rigidity of Robot Structure: Analysis and Enhancement", Proc. 1985 Amer. Cont. Conf., Boston, Mass., June 1985.
[18] P.D. Atherton, et al, "An Infinitely Stiff Very High Precision Actuator, Proc. of the 1987 Precision Engineering Conference, Cranfield UK.
[19] J.R. Leteurte, "Capacitance Based Sensing and Servo Control to Angstrom Resolution", Proc. of the 1987 Precision Engineering Conference, Cranfield UK.

Table 1 Properties of various materials and relative time for temperature change in a 1m diameter inner sphere caused by disturbance of 0.001°C in the outer temperature control envelope to cause 0.1Å thermal expansion in a 0.25m segment[1]

Material	ρ (kg/m^3)	E (Gpa)	$\alpha_{expansion}$ ($\mu m/m\text{-}^oK$)	K ($w/m\text{-}^oK$)	C_p ($J/Kg\text{-}^oK$)	t (secs)	ΔT ($^oCx10^{-6}$)	α ($m^2/sx10^{-6}$)
Aluminum	2707	69	22.0	231	900	130	1.8	94.8
Beryllium	1848	275	11.6	190	1,886	352	3.4	54.5
Copper	8954	115	17.0	398	384	237	2.3	116
Grey cast iron	7200	80	11.8	52	420	300	3.4	17.2
Invar	8000	150	0.9	11	515	5533	44.4	2.7
Lead	11373	14	26.5	35	130	65	1.5	23.7
Zerodur	2550	90	0.15	6	821	22,733	266	2.9

[1]For the small temperature excursions considered here, the time t is proportional to the diameter of the sphere and inversely proportional to the temperature excursion of the outer sphere.

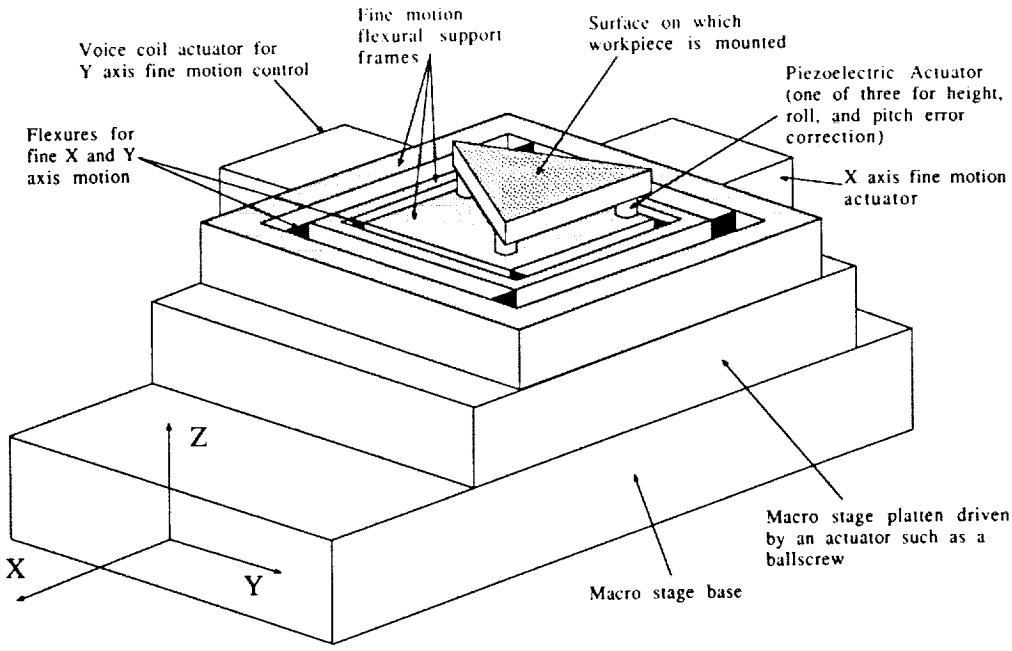

Figure 1 Example of a coarse-fine positioning system used to correct for slide errors caused by errors in slide geometry and forces caused by a misaligned actuator

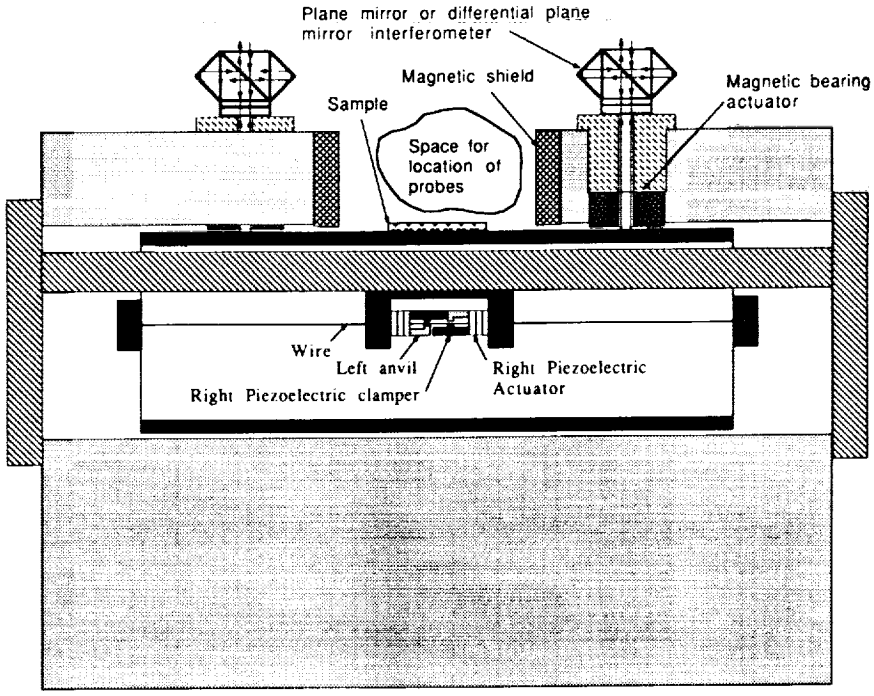

Figure 2 Cutaway side view of Atomic Resolution Measuring Machine (ARMM)

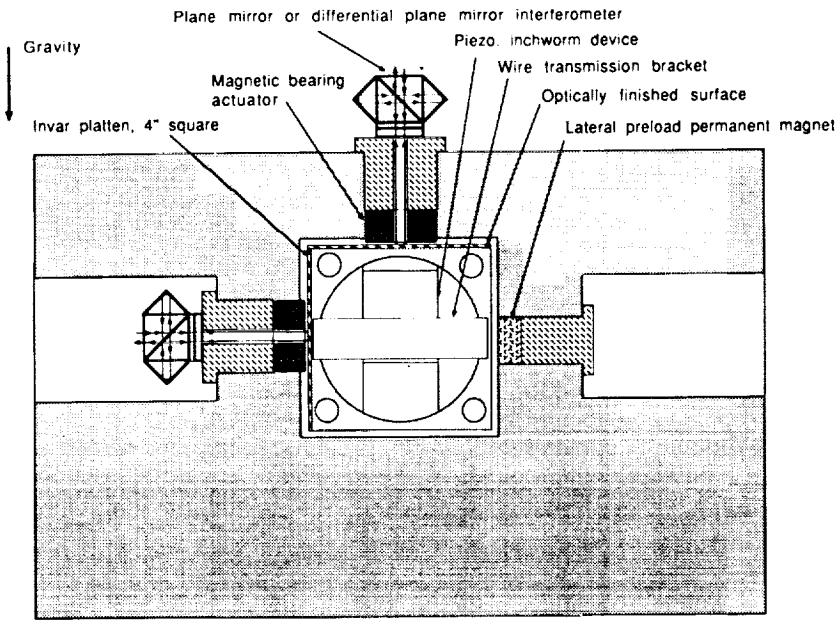

Figure 3 Cutaway right end view of Atomic Resolution Measuring Machine (ARMM)

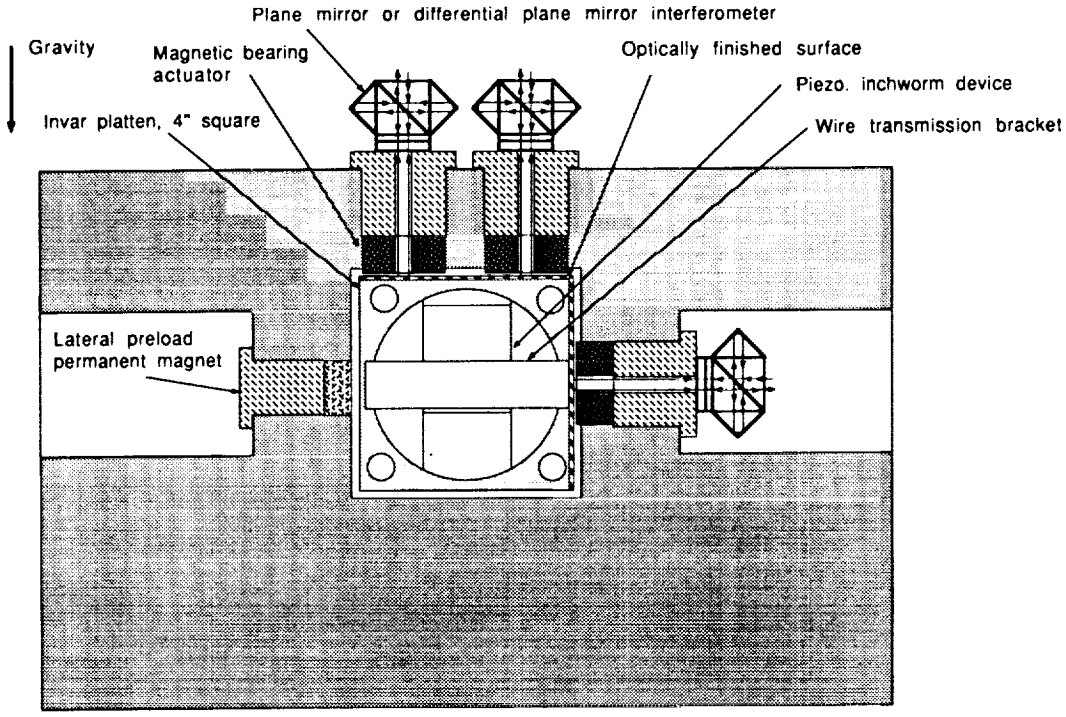

Figure 4 Cutaway left end view of Atomic Resolution Measuring Machine (ARMM)

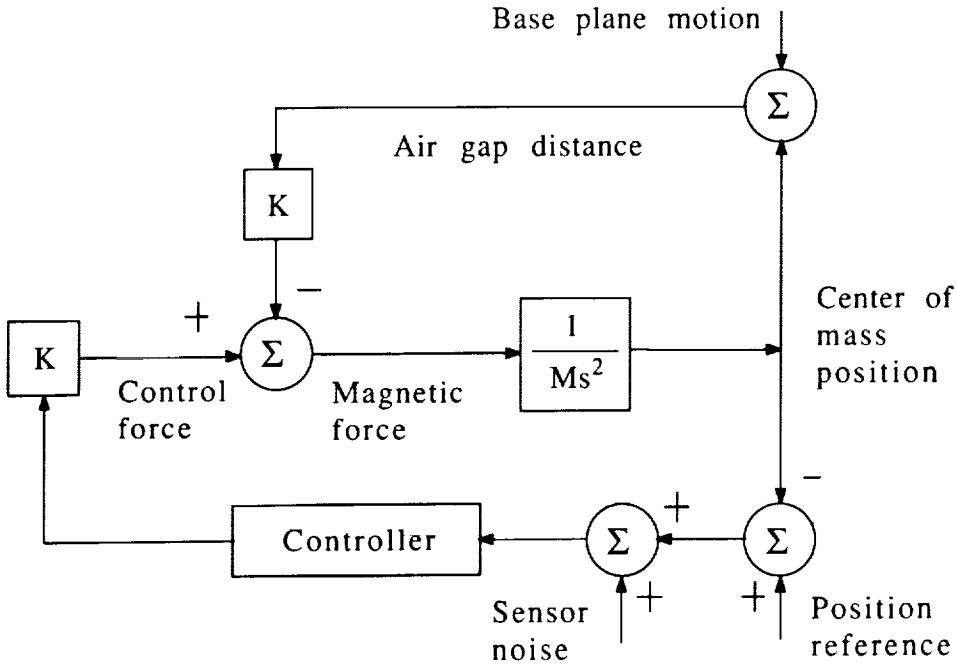

Figure 5 Basic magnetic suspension block diagram

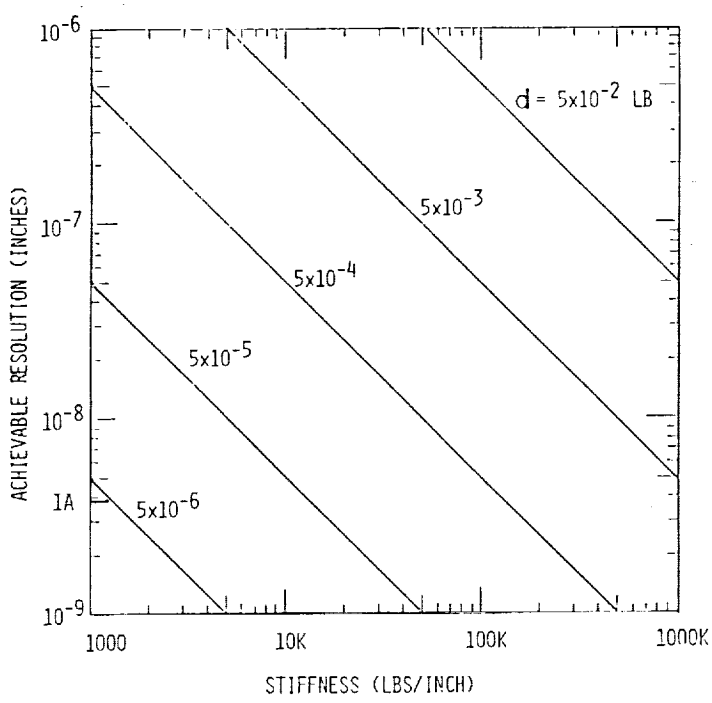

Figure 6 Achievable suspension resolution vs. suspension stiffness

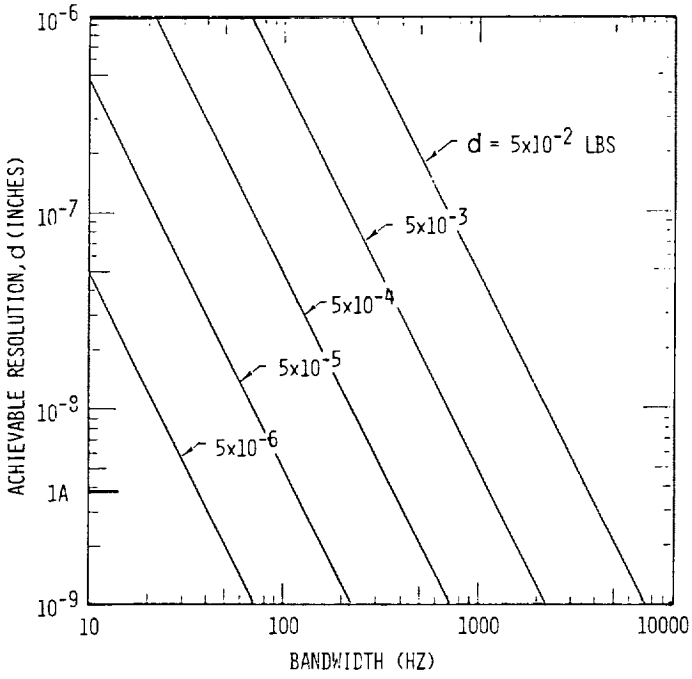

Figure 7 Achievable suspension resolution vs. suspension stiffness

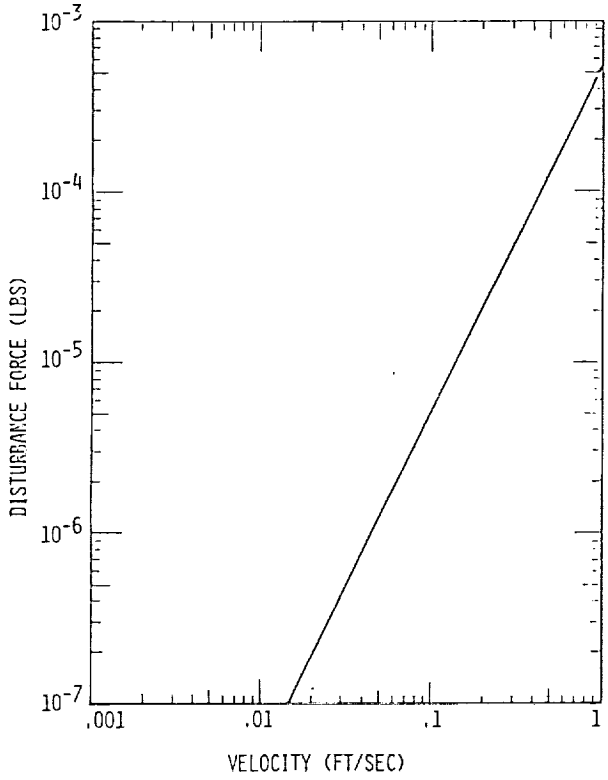

Figure 8 Slide disturbance force as a function of impinging air flow

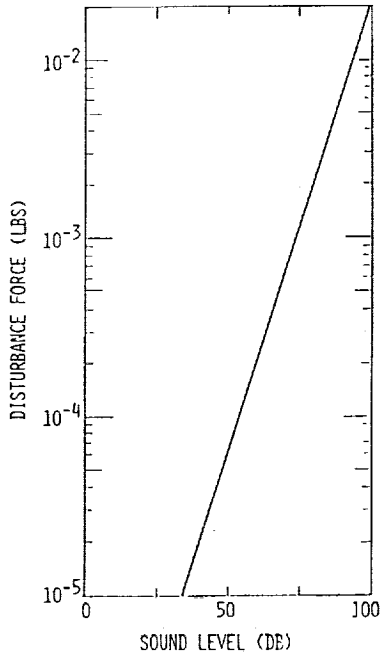

Figure 9 Slide disturbance force vs. acoustic noise level

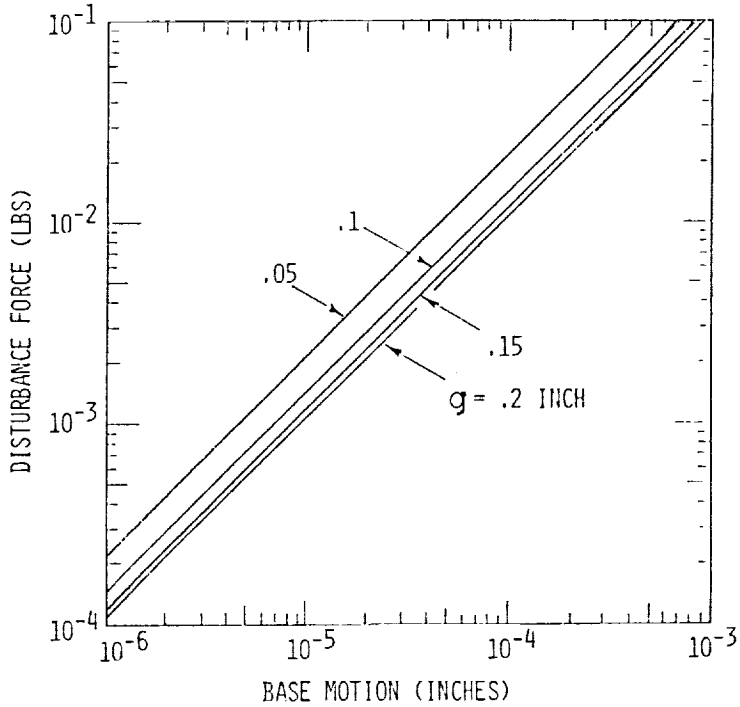

Figure 10 Slide disturbance force as a function of base plane motion

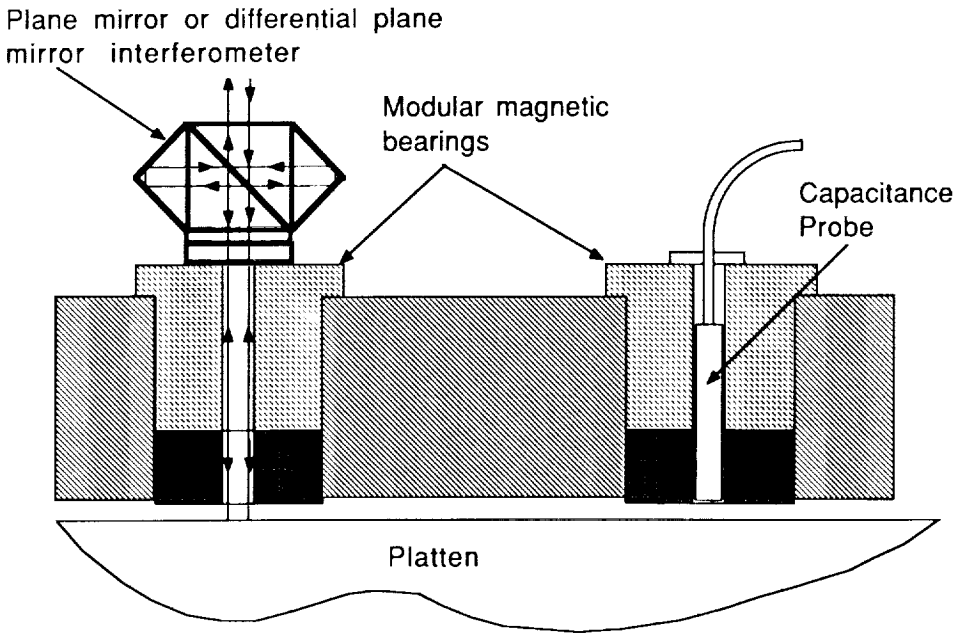

Figure 11 Possible sensor arrangements for precision "through the bearing measurement"

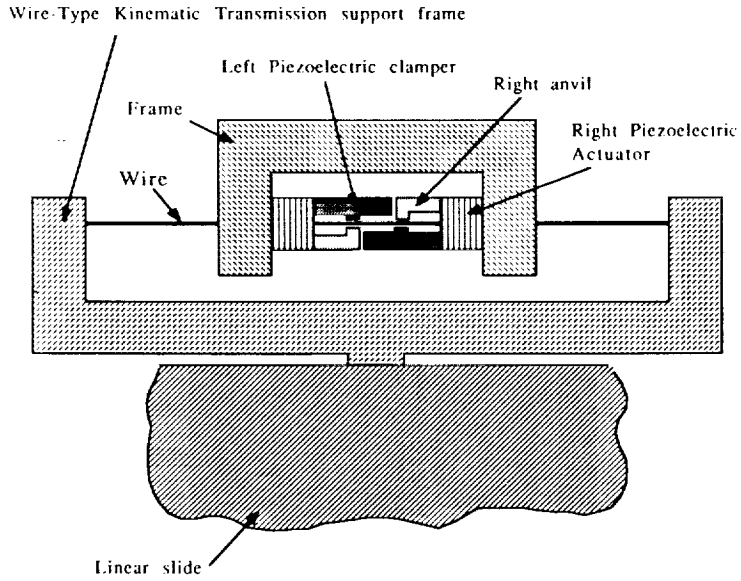

Figure 12 Schematic design of the Wire-Type Kinematic Transmission/Piezoelectric Inchworm Actuator designed for the Molecular Measuring Machine

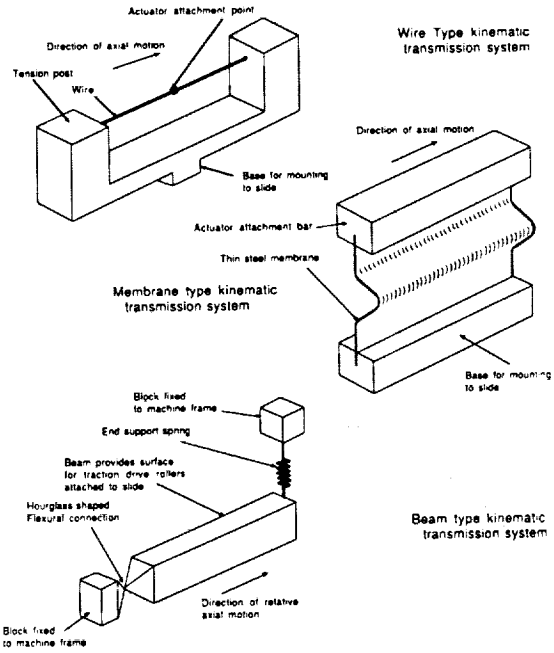

Figure 13 Types of flexural kinematic transmissions

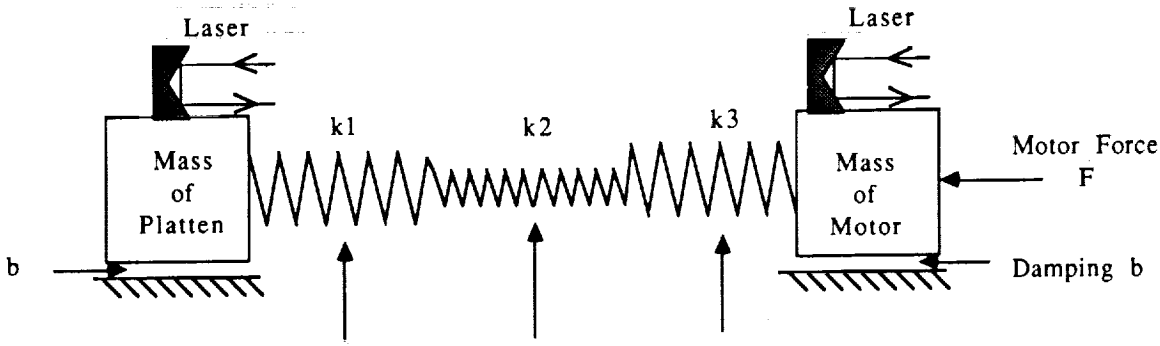

$$\frac{1}{k1} + \frac{1}{k2} + \frac{1}{k3} = \frac{1}{k} \approx \frac{1}{k2}$$

Figure 14 Dynamic system model of a wire-type kinematic transmission